The Journal of Korean Vacuum Science & Technology
Vol. 3, No. 2, October 1999, pp. 107~111

Experimental response function of a phtoelectron spectrometer

Moonsup Han, Hye-Yeong Shin* and S.-J. Oh*

Department of Physics, The University of Seoul, Seoul 130-743, Korea
**Department of Physics, Seoul National University, Seoul 151-742, Korea*
(Received October 18, 1999)

Abstract – We developed the experimental response function (ERF) which can be used for the numerical curve fitting analysis in photoelectron spectroscopy (PES). We selected the core-levels of Ag $3d_{5/2}$ and Au $4f_{7/2}$ to obtain the ERF because the parameters characterizing the intrinsic line-shape have been known well. Relying on the numerical fourier transformation we deconvoluted the ERF from the measured core-level spectra. For the numerical fourier transformation we applied the fast transform (FFT) algorithm. We considered optimal (Wiener) filtering with the FFT due to noise and used Hann window function to remedy the information leakage in frequency domain due to discrete and finite sampling of measurement. The comparison of the curve fitting results using the ERF obtained in this work and the mathematical response function with a gaussian in the conventional approach shows clearly the improvement of the curve fitting analysis.

I. Introduction

The electron is widely used to probe various physical and chemical properties of solid state materials. Among the spectroscopic methods is the photoelectron spectroscopy (PES) a well-established and powerful tool to study electronic structures of the bulk or the surface of solids [1]. The energy-distribution curve (EDC) of PES is closely related with the electronic level density of states of solid systems. In order to interpret the electronic structure of a solid from the photoelectron spectra we must throughly analyze overall effects on the spectral line-shape. Many researchers proposed early the "three step model" [1, 2] in which the photoemission process is explained by the sequences of 1) the optical excitation of a bound electron in an elastic scattering with photons, 2) the transport of the electron throughout the solid, and 3) the escape through the surface-potential barrier of the sample into the vacuum. These are represented as the distribution of photoexcited electrons $p(E, \omega)$, the transmission function of $t(E, \omega)$, and the escape function $d(E, \omega)$ as the following:

$$I_e(E, \omega) = p(E, \omega) \times t_e(E, \omega) \times d(E, \omega) \qquad (1)$$

where the E denotes the kinetic or binding energy of photoelectron and the photon source energy is $\hbar\omega$. Here we consider only the photoexicited electrons with no loss of energy i.e. elastic process as presented with the subscript "e". The background due to the inelastic scattering is independently treated when the spectrum is analyzed. Since the photoelectron spectrometer is mainly composed of photon source, sample, and electron analyser, the convolution of all these factors is proceeded to make an experimental spectrum. To extract the intrinsic signal $p(E, \omega)$ of a sample from the energy-distribution curve $c(E, \omega)$ of real spectrum by numerical deconvolution, one assumes that all the instrumental and/or the extrinsic factors can be represented by a response function $g(E, \omega)$. Considering the convolution of the intrinsic signal function $p(E, \omega)$ and the instrumental response function $g(E, \omega)$, we have the experimental signal function c(E, ω) as the following;

$$c(E) = \int p(E - E') \cdot g(E') dE'. \qquad (2)$$

Here we omitted the photon source frequency ω because the photon energy is normally fixed in the experiment. For the core-level spectrum in x-ray photoelectron spectroscopy (XPS), the Doniach-Šunjić (DS) line-shape is a well known function for metallic system [3-5]. It consists of a lifetime-broadened Lorentzian and the successive modification by the immediate excitation of conduction-electrons around the fermi sea which makes an

influence on the asymmetric line-shape in lower kinetic energy range of the spectrum.

On the other hand, the principal factors of the extrinsic (i.e. instrumental) broadening are from photon source and analyser transmission. Many researchers have used conventionally a single gaussian function as the response function. This assumption is inappropriate for the precise line-shape analysis since the actual response function including overall instrumental factors such as photon source, analyser transmission, temperature, etc. does not have the shape of gaussian function [6]. Therefore the conventional curve fitting with a mathematical gaussian function as the instrumental response function [7, 8] might mislead uncorrect information.

In this work, we present a method to obtain the experimental response function (ERF) for photoelectron spectrometer. The ERF can be used to extract the intrinsic contribution of sample itself from the spectrum of photoelectron spectroscopy. For the purpose of exploring the ERF we applied the deconvolution method with numerical fourier transformation for a discrete data set of the XPS experiment [9-11].

II. Experiments

We used a photoelectron spectrometer manufactured by VSW Scientific Instruments Ltd. The spectrometer has been equipped with the 150 mm-radius concentric hemispherical analyser and the multichannel detector system. We selected the polycrystalline plates of Ag and Au as samples. Their thickness were smaller than 1 mm. The sample surface was cleaned by mechanical polishing before inserting into ultra high vacuum (UHV) chamber, and by scrapping with the diamond file or by the argon sputtering *in vacuo*. The cleanness of the samples was inspected by checking oxygen and carbon 1*s* peaks in XPS spectrum. Very little oxygen and carbon contaminations were detected. The core-levels we selected for the analysis were Ag $3d_{5/2}$ and Au $4f_{7/2}$ because the parameters characterizing the intrinsic line-shape such as the Lorentzian width and the singularity index (asymmetry parameter) have been known well.

For each sample, the experiment was performed by varying the fixed analyser transmission (FAT) energy with 10 eV, 22eV, and 44 eV for two x-ray photon sources Al K_α line ($h\nu$ = 1486.6 eV) and Mg K_α line ($h\nu$ = 1253.6 eV). These various measurements enable us to extract more reliable information on the ERF of the spectrometer. The experimental data were taken in enough energy range for Ag 3*d* and Au 4*f* spin-orbit peaks with the energy increment 0.08 eV and the data acquisition time 250 msec a each step. During the experiment, the base pressure was maintained in the range of 3×10^{-10} mbar ~1.5×10^{-9} mbar.

III. How to obtain ERF

For conventional formula development, we use t parameter instead of E for energy because we control kinetic or binding energies in time domain during data acquisition. In fourier transformed space, we can write the energy distribution curve as the following

$$C(f) = P(f) \cdot G(f) \tag{3}$$

where the capital functions are the inverse fourier transformed functions of the original ones, and the parameter f denotes the frequency which is conjugate to the time t in the fourier transformation. Since we know the intrinsic signal function $p(t)$ from the literature [12] and measure the energy distribution function $c(t)$ in experiment, we can evaluate numerically the inverse fourier transformed instrumental response function $G(f)$ from Eq. (3). Also we can easily obtain the ERF $g(t)$ by the inverse fourier transformation. This instrumental response function we want to get is independent of the measured samples. It must be singly determined for one experimental setup which includes the selection of photon source and the pass energy of the analyser transmission excluding intrinsic sample parameters. The instrumental or extrinsic factors only determines the response function.

For the numerical fourier transformation we use the algorithm of the fast fourier transformation (FFT) which reduce the computational load to $O(N \log_2 N)$ from $O(N^2)$ when the number of data points is N [13, 14]. Practically, it is unavoidable to include the noise spectral weight in the experimental spectrum. To remove the effect of noise on the fourier transformed function in FFT, we used the optimal

(Wiener) filtering which is generally used [14]. On the other hand, since the discrete and finite sampling of the measurement also modifies the result of the transformation it is necessary to remedy the information leakage by the data windowing. We used "Hann window function" as the data windowing function. All the values the data points are multiplied by a value of the window function at each point before performing FFT. The usefulness of this experimental response function in the line-shape analysis will be shown in the next section.

IV. Results and Discussion

The following procedure was applied to all spectra we obtained. Since we used unmonochromatic photon source we corrected x-ray satellites with the known position and intensity ratios of satellites for Mg and Al K_α lines. For the background correction due to inelastic scattering of photoexcited electrons, we used the integral (or Shirley) method [15]. The background line was optimized by least-square fitting. Since it is enough to choose one from double peaks of spin-orbit splitting for Ag 3*d* and Au 4*f* core-levels, we subtracted the higher intensity peaks Ag $3d_{5/2}$ and Au $4f_{7/2}$ by conventional curve fitting using mathematical response function (single gaussian function). This procedure was iteratively corrected after obtaining the numerical response function. We say this result the experimental signal function $c(t)$ for the core-level. We like to start from this function to obtain ERF. As we introduced, this experimental signal function $c(t)$ is originated from convolution of the intrinsic signal and the experimental response functions. Here we assumed that the shape of the intrinsic signal for the core-levels follows the DS line-shape with the Lorentzian width and asymmetry parameters according to those of Wertheim's early work [12]. The Lorentzian width and the asymmetry parameters for Ag 3*d* are known to be 0.281 eV and 0.059, respectively and those for Au 4*f* are 0.329 eV and 0.048, respectively.

Before performing the fourier transformation of the experimental signal function $c(t)$ we applied Hann window as we mentioned in the previous section. After the transformation of the Hann-windowed data-set, we obtained the power spectral density (PSD) which is the squared amplitude function at each frequency [14]. Figure 1 shows the PSD functions for (a) Ag $3d_{5/2}$ and (b) Au $4f_{7/2}$. Here $C(f)$ denote the experimental signal function disturbed by the noise function $N(f)$ and $S(f)$ the pure signal function excluding the noise effect in the frequency domain. Assuming the pure signal function and the noise function in frequency domain as the straight lines as shown in the figure, we obtained the optimal (Wiener) filtering function $\Phi(f)$ to remove noise effect. The hand-waving decomposition of the pure signal and noise function in PSD is enough to get the optimal (Wiener) filtering function.

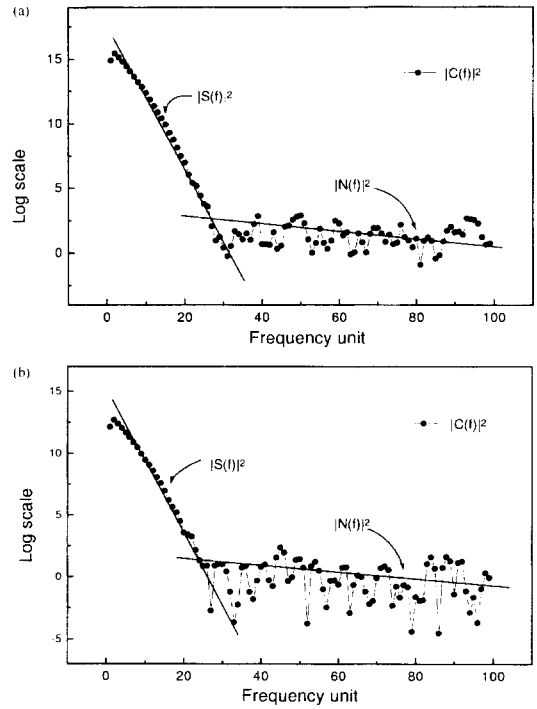

Fig. 1. Power-spectral-density (PSD) functions for (a) Ag $3d_{5/2}$ and (b) Au $4f_{7/2}$. $C(f)$ denotes the experimental signal function disturbed by noise function $N(f)$ and $S(f)$ the pure signal function excluding the noise effect in the frequency domain.

We can easily obtain the fourier transformed intrinsic signal $P(f)$ from the DS line-shape function with the known parameters. We finally determine the numerical response function in frequency domain as the follwing;

$$G(f)=\frac{C(f)\Phi(f)}{P(f)} \tag{4}$$

We note that $G(f)$ in Eq. (4) is the noise corrected

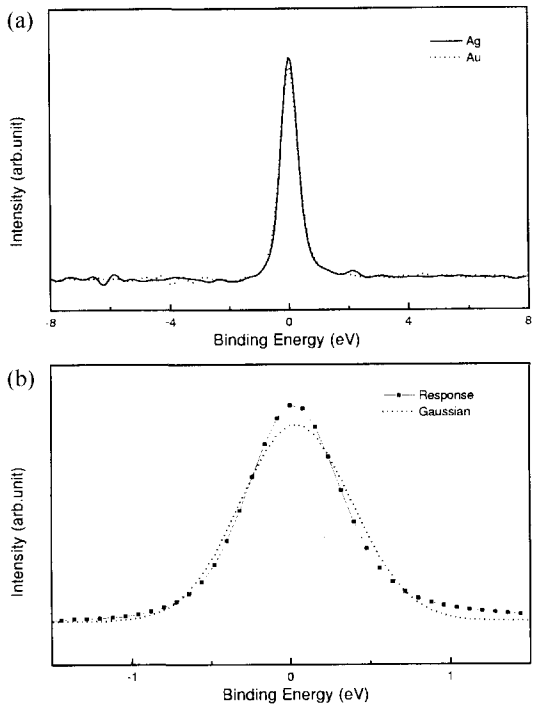

Fig. 2. (a) The experimental response functions (ERF's) from the analysis of Ag 3*d* (solid line) and Au 4*f* (dotted line) core-levels with the same experimental setup of Mg K_α photon source and FAT 22 eV. (b) The magnified average function (solid line) of the experimental response functions for Ag and Au and the best-fit gaussian function for the ERF (dotted line) obtained in this work.

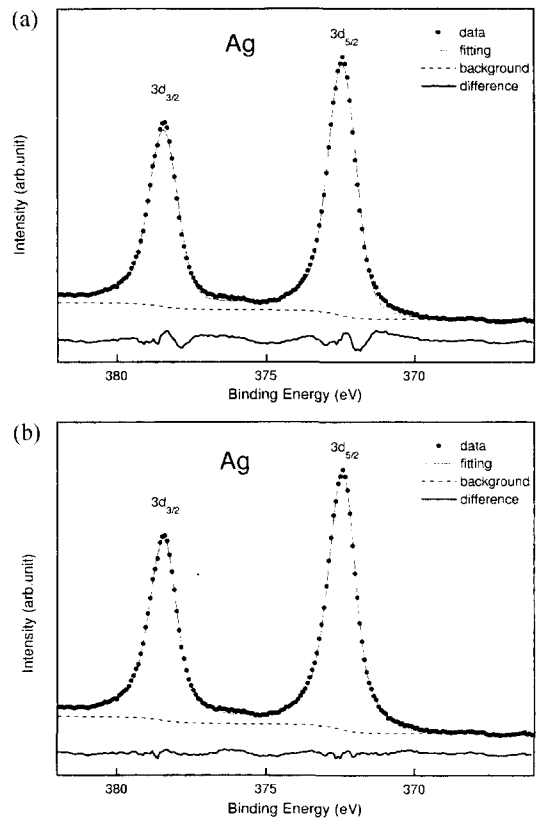

Fig. 3. The curve fitting result for the Ag 3d core-level using (a) the mathematical single gaussian, and (b) the newly obtained experimental response function as the instrumental response functions, respectively.

function by the optimal filtering function which is slightly different from the one in Eq. (3). The experimental response function $g(t)$ in real space can be determined by inverse fourier transformation of $G(f)$. Figure 2(a) shows ERF's from the analysis of Ag 3*d* (solid line) and Au 4*f* (dotted line) core-levels with the same experimental setup of Mg K_α photon source and FAT 22 eV. Since the ERF is independent of samples, the ERF's from Ag and Au should be same. Those in Fig. 2(a) look very same with the consideration of experimental resolution. Therefore we determined the ERF as the average function of those. Figure 2(b) shows the average function (solid line) of the ERF's for Ag and Au and the best-fit gaussian function for the ERF (dotted line) obtained in this work. As we expect the difference between two function in Fig. 2(b) is considerable which causes the failure of the conventional curve fitting with the instrumental response function as a mathematical single gaussian as shown in Fig. 3(a) and Fig. 4(a) for Ag 3*d* and Au 4*f*, respectively. We see cleary the improvement of the curve fitting result when we apply the ERF for the core-levels of Ag 3*d* and Au 4*f* as shown in Fig. 3(b) and 4(b), respectively. In Fig. 3 and Fig. 4, we extend the fitting range to include both spin-orbit peaks with same parameters except the intensity ratios between those. We see also that the typical wobbling of the residual around the center of peak in the conventional fitting is considerably reduced in the new one of this work.

V. Conclusions

We developed the experimental response function which can be used for the numerical curve fitting

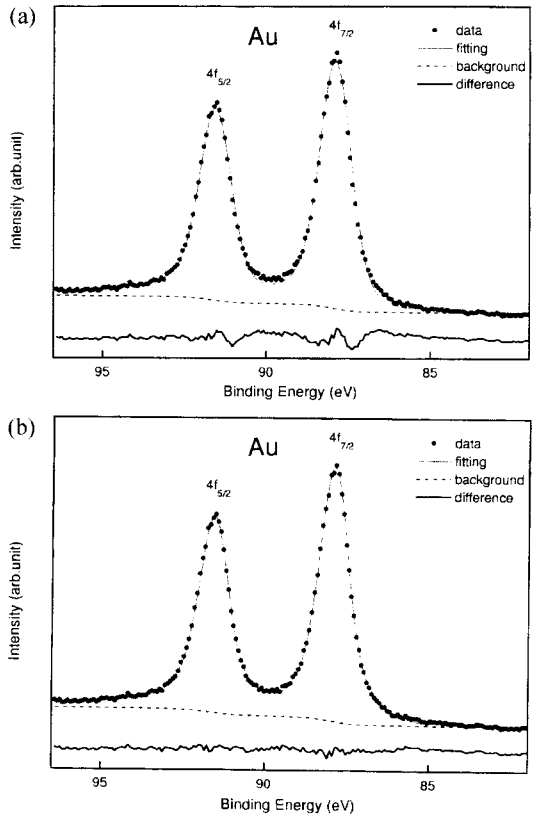

Fig. 4. The curve fitting result for the Au 4f core-level using (a) the mathematical single gaussian, and (b) the newly obtained experimental response function as the instrumental response functions, respectively.

analysis in PES. Using the numerical fourier transformation with the fast transform (FFT) algorithm we deconvoluted the ERF from the measured core-level spectra. We considered optimal (Wiener) filtering with the FFT due to noise and used Hann window function to remedy the information leakage in frequency domain due to discrete and finite sampling of the measurement. The comparison of the curve fitting results using the ERF obtained in this work and the mathematical response function with a gaussian in the conventional approach shows clearly the improvement of the curve fitting analysis.

With this ERF obtained in this work, it is expected that we can more exactly perform the curve fitting for the photoelectron spectra.

Acknowledgments

The author (M. Han) acknowledges Mr. M.-C. Jung and J.-W. Park for the help preparing figures in this manuscript. This work was supported by the Basic Science Research Institute Program, Ministry of Education (BSRI-98-2416).

References

[1] S. Hüfner, *Photoelectron Spectroscopy: Principles and Applications* 2nd Ed., (Springer-Verlag, Berlin, 1996); Ed. by L. Ley, M. Cardona, *Photoemission in Solids I*, Topics Appl. Phys. Vol. 26 (Springer-Verlag, Berlin, 1979); Ed. by L. Ley, M. Cardona, *Photoemission in Solids II*, Topics Appl. Phys. Vol. 27 (Springer-Verlag, Berlin, 1979).

[2] C. N. Berglund and W. E. Spicer, *Phys. Rev.* A **136**, 1030; 1044 (1964).

[3] S. Doniach and M. Šunji, *J. Phys. C. Solid State Phys.* **3**, 285 (1970).

[4] N. Martenson, R. Nyholm, H. Caleén, J. Hedman, and B. Johansson, *Phys. Rev.* B **24**, 1725 (1981).

[5] R.S. Rao, A. Bansil, H. Asonen, and M. Pessa, *Phys. Rev.* B **29**, 1713 (1984).

[6] H. Felner-Feldegg, U. Gelius, S. Wannberg, A.G. Nilsson, E. Basilier and K. Siegbahn, *J. Electron Spectroscopy* **5**, 643 (1974).

[7] H. C. Burger and P. H. van Cittert, *Z. Physik*, **79**, 722 (1932); *ibid* **81**, 428 (1933).

[8] P. A. Jansson, "*Deconvolution with Application in Spectroscopy*" Academic Press (1986).

[9] H. Busse, K. Wandelt, and G.R. Castro, *J. El. Spec. Relat. Phenomena* **72**, 311 (1995).

[10] P. E. Siska, *J. Chem. Phys.* **59**, 6052 (1973).

[11] S. Lawrence Marple, Jr., "Digital Spectral Analysis with application" Chap. 2, Prentice Hall (1987).

[12] P. H. Citrin and G. K. Wertheim, *Phys. Rev.* A **27**, 3160 (1983).

[13] D. B. Percival and A. T. Walden, "Spectral Analysis for Physical Applicaions" Chap. 3 Cambridge University Press (1993).

[14] W. H. Press, B. P. Flannery, S. A. Teukolsky and W. T. Vetterling, "Numerical Recipes in C", Cambridge University Press (1989).

[15] D. A. Shirley, *Phys. Rev.* **5**, 4709 (1972).